Fabrication of Nano-wrinkled Silsesquioxane-based Nanostructures by Coupling Polymeric Surface onto Rigid Templates Assembled from Unique Deca-silsesquioxane

Jun Peng,[†, ‡] Yuxiu Xing,[†, ‡] Weihong Lin,[†, ‡] Kai Xu,*[,†] Jiancheng Wu,[†, ‡] Zhiwei Yu,[†, ‡] Youxiong Zhang, [†, ‡] and Mingcai Chen[†]

[†]Guangdong Provincial Key Laboratory of Organic Polymer Materials for Electronics, Guangzhou Institute of Chemistry, Chinese Academy of Sciences, P. O. BOX 1122, Guangzhou 510650, People's Republic of China.

[‡] University of the Chinese Academy of Sciences, Beijing 100049, People's Republic of China.

KEYWORDS silsesquioxane cages; self-assembly; compressive stress; nano-wrinkled structures; antireflection surface

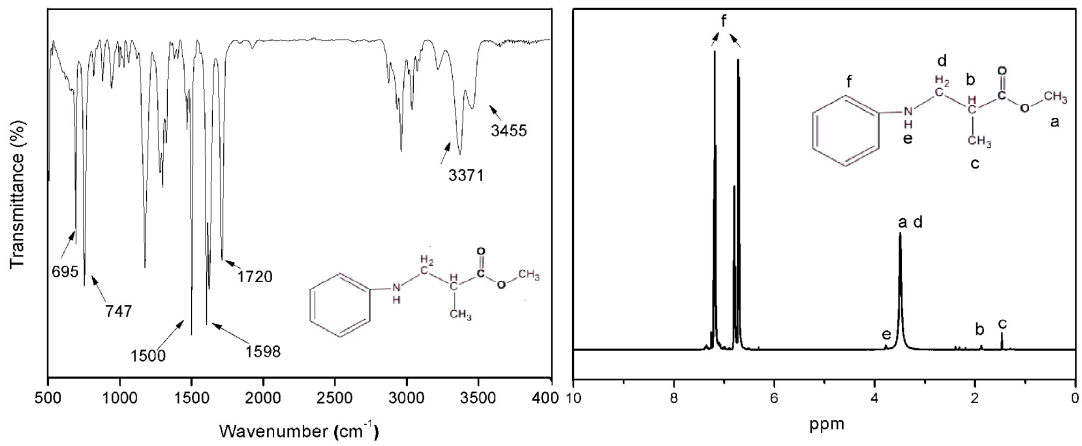

Figure S1. FTIR and ¹H NMR (in $CHCl_3$-*d*) of the model experiment product of methylmethacrylate reacted with aniline.

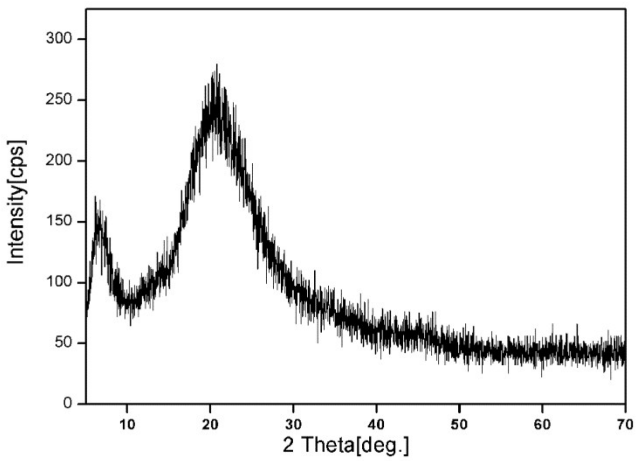

Figure S2. XRD spectrum of the bulk layer coating film comprising OASQ and CMSQ-T_{10} (molar ratio =1:8) .

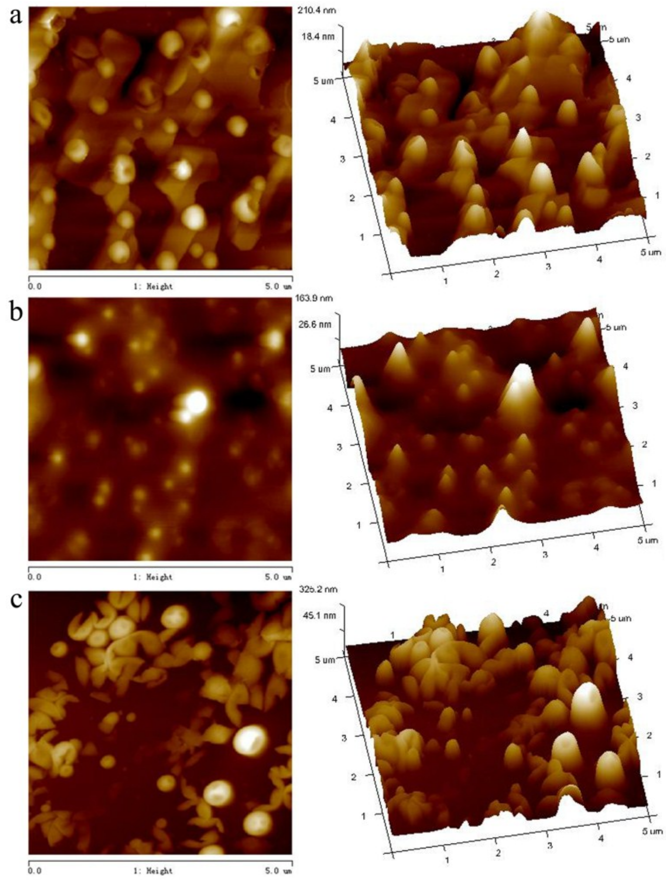

Figure S3. AFM height image and 3D image of the bulk layer consisting of OAPS and CMSQ-T_8 in a molar ratio of 1:8 (a), 1:4 (b), 1:1 (c).

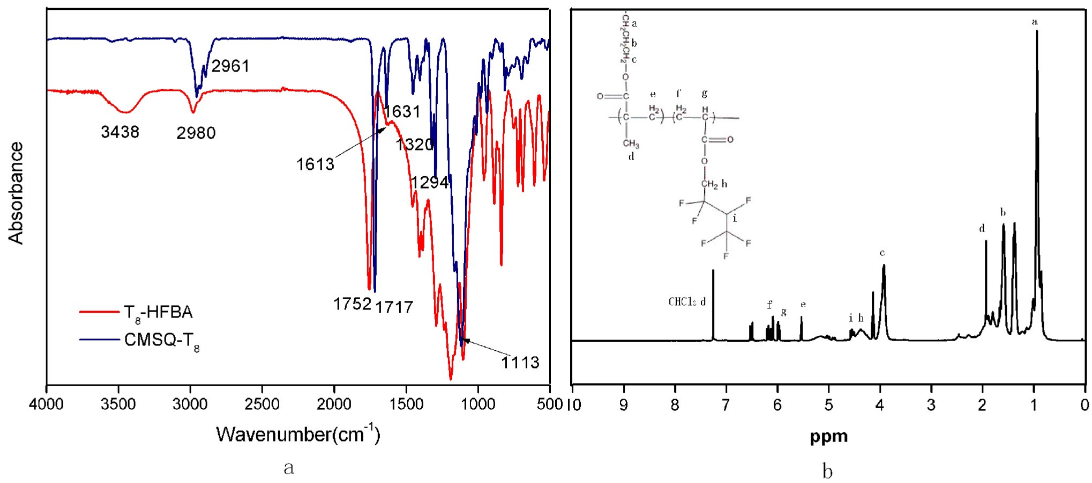

Figure S4. FTIR and ^{1}H NMR (in $CHCl_3$-*d*) of the product of CMSQ-T_8 reacted with hexafluorobutyl acrylate.

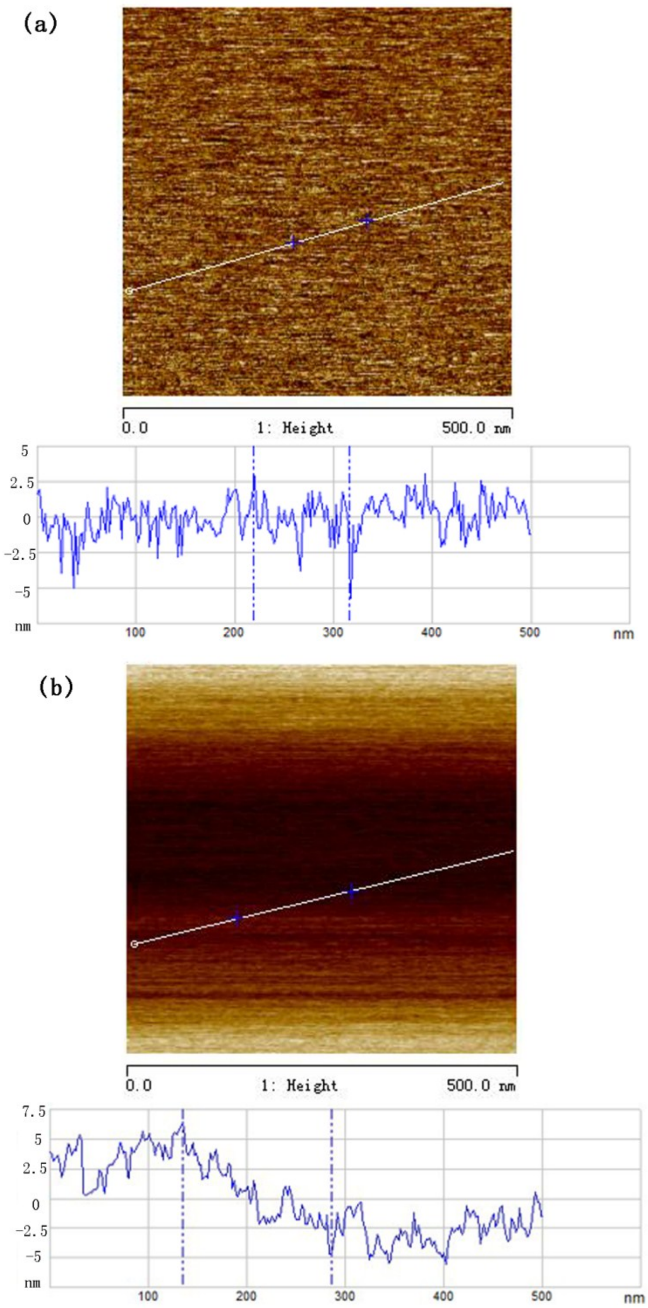

Figure S5. AFM height images of STL coating with the formulation of CMSQ-T_8 and hexafluorobutyl acrylate in a mass ratio of 1:100 (a) and double-layer coating with the formulation of octakis(aminophenyl) silsesquioxane and CMSQ-T_{10} in a molar ratio of 1:8 for template layer and CMSQ-T_8 and hexafluorobutyl acrylate in a mass ratio of 1:100 for top layer (b). (A typically sample to obtain the characteristic wavelength (λ) and amplitude (A), othe and so on)

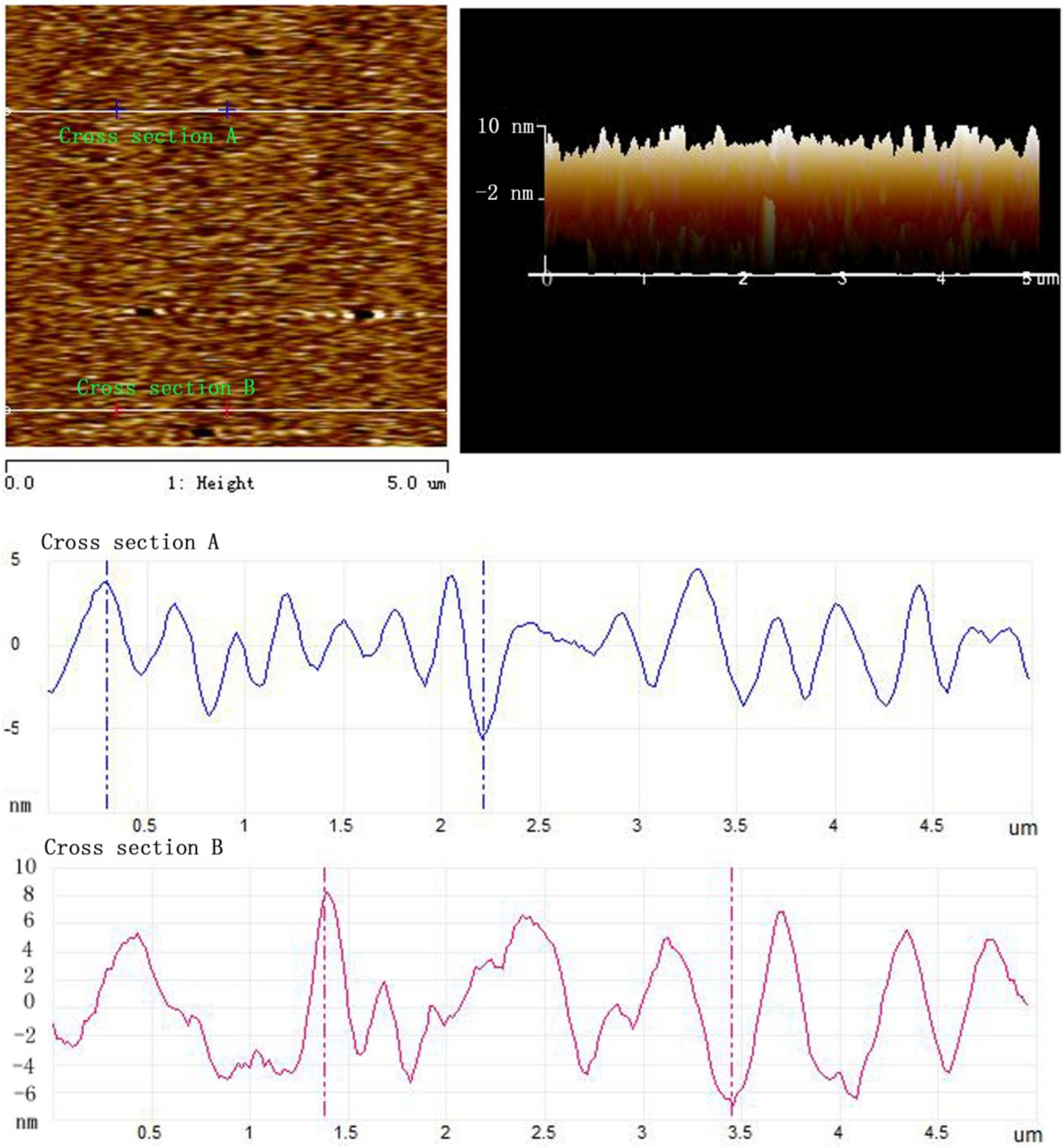

Figure S6. Lateral profile and cross section analysis of the obtained double-layer nano-wrinkled surface (octakis(aminophenyl) silsesquioxane and CMSQ-T10 in a molar ratio of 1:8 for template layer and CMSQ-T8 and hexafluorobutyl acrylate in a mass ratio of 1:100 for top layer)

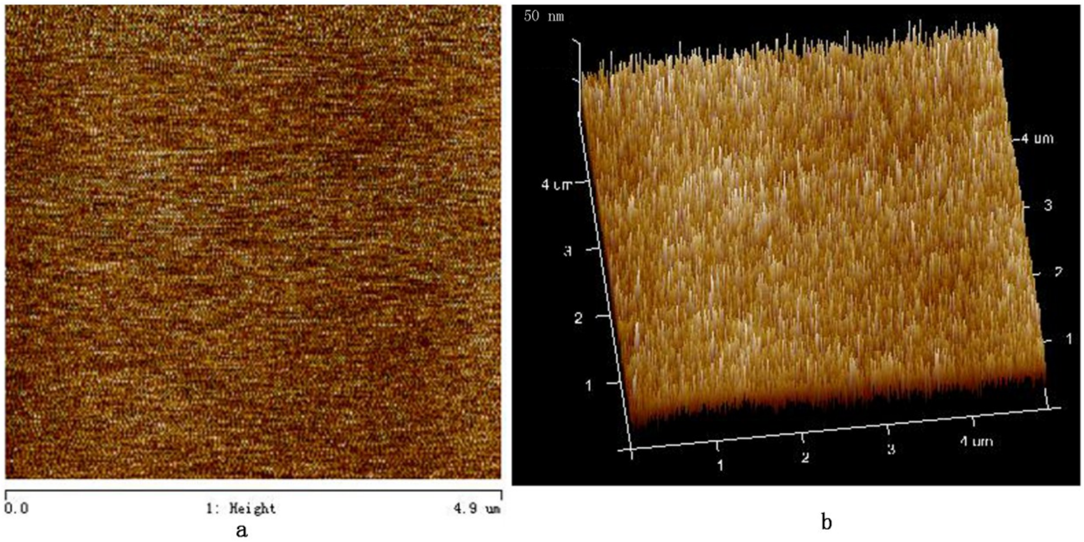

Figure S7. AFM height image (a) and 3D image (b) of the double-layer surface with the formulation of octakis(aminophenyl) silsesquioxane and CMSQ-T_{10} in a molar ratio of 1:8 for bulk layer and hexafluorobutyl acrylate for top layer.

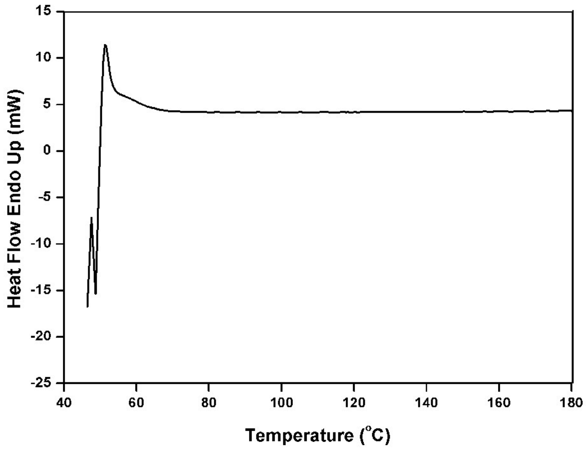

Figure S8. DSC spectrum of the template layer mixture (hydroquinone was used as double-bond addition reaction inhibitor).

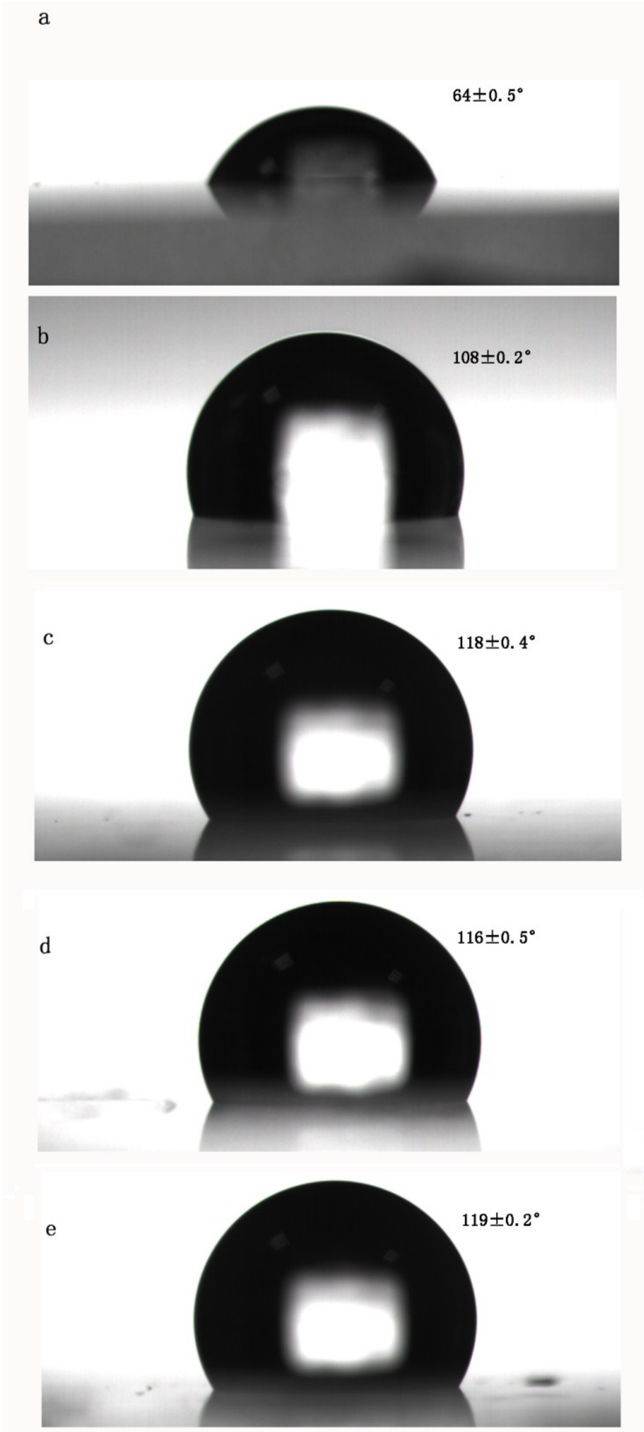

Figure S9. WCA on various quartz glass surfaces measured immediately after treatment (a) pristine quartz glass, (b) coated STL coating with the formulation of CMSQ-T_8 and hexafluorobutyl acrylate in a mass ratio of 1:100, (c) coated the DLS-8, (d) coated the DLS-4 and (e) coated the DLS-1.

Table S1. Roughness analysis results of STL and double-layer coating surface.

	Image Rq (nm)	Rq (nm)	Image Ra (nm)	Ra (nm)
STL Coating	2.01	2.01	1.75	1.75
Double-layer coating	3.11	3.11	2.10	2.10

Image Rq, Ra represents root mean square average of height deviations taken from the mean image data plane and Arithmetic average of the absolute values of the surface height deviations measured from the mean plane, respectively; Rq, Ra is the standard deviation of the Z values within the box cursor and Arithmetic average of the absolute values of the surface height deviations measured from the mean plane within the box cursor.

Table S2. n, k of the antireflection coating film that the simulation needed which were obtained by using the ellipsometer

Incident light wavelength: 550 nm			
	n	k	thickness
Template layer	1.699185	0.168870	46.7 ±0.4 nm
Top layer	1.700559	0.157419	151.2±0.5 nm

Table S3. Contact angle and surface energy of the STL coating and Double-layer coatings.

Series	water	n-hexadecane	surface energy
	θ_{staic}, deg	θ_{staic}, deg	(mN/m)$^{\alpha}$
STL coating	108±0.2	63±0.2	15.6±0.5
DLS-1	119±0.2	76±0.5	11.0±0.3
DLS-4	116±0.5	71±0.2	12.4±0.1
DLS-8	118±0.4	74±0.4	11.3±0.1

$^{\alpha}$Calculating from water contact angle and n-hexadecane contact angle by means of Owens method. θ_{staic} is static contact angle.